A MECHANISM-BASED RANDOM FIELD PROJECTION FOR STOCHASTIC ANALYSIS OF CONCRETE STRUCTURES AND OTHER QUASIBRITTLE STRUCTURES

JIA-LIANG LE[*] AND JOSH VIEVERING[‡]

[*] Department of Civil, Environmental, and Geo- Engineering, University of Minnesota
Minneapolis, MN, 55445, USA
e-mail: jle@umn.edu

[†]Department of Civil, Environmental, and Geo- Engineering, University of Minnesota
Minneapolis, MN, 55445, USA
e-mail: vieve005@umn.edu

Key words: Stochastic Finite Element, Random Fields, Mesh Dependency, Damage Localization

Abstract. This study investigates the mathematical algorithm for mapping the continuous random fields of material properties onto the FE meshes, and its implications for the mesh sensitivity in stochastic FE analysis of quasibrittle fracture. We adopt a continuum damage constitutive model, and develop a mechanistic mapping method. The projection of the random fields of material properties onto the FE mesh is governed by the prevailing damage pattern of the finite element. The model is applied to stochastic FE analysis of notched and unnotched flexural specimens under different loading configurations. The numerical analysis also considers different correlation lengths of the random fields of material properties. The simulation shows that, even with the proper energy regularization scheme, the commonly used local mapping and local average methods could yield considerable mesh dependence of the peak load statistics. By relating the mapping algorithm to the underlying damage pattern, the present model is able to mitigate the mesh sensitivity for different specimen geometries, loading configurations, and correlation lengths.

1 INTRODUCTION

Due to the inherent uncertainties in applied loads and structural resistance, reliability analysis is crucial in the design of various engineering structures. In the past two decades, significant attention has been given to structures made of quasibrittle materials, such as concrete, ceramics, fiber composites, rock, and cold asphalt. Although several analytical models have been developed to understand the failure statistics of quasibrittle structures [1–3], the stochastic finite element method (SFEM) remains the most versatile approach for evaluating the probability distribution of load resistance.

The Monte Carlo simulation (MCS) is arguably the most widely used approach for SFEM. Generally, MCS involves two steps: 1) the mathematical representation of spatially distributed random material properties and 2) the numerical simulation of nonlinear structural response. The spatial randomness of the material properties is conveniently described by homogeneous random fields. To complete the MCS scheme, the continuous random field of material properties needs to be mapped onto the FE mesh. In SFEM, two methods have been widely used: 1) direct local projection [4], where the value of the random constitutive parameter of

the finite element is taken directly from the underlying field at the element's centroid, and 2) local averaging, where the random constitutive parameter of the finite element is determined by averaging the corresponding random field over the element's domain [4–6]. However, from a physical perspective, these methods are questionable for the strength and fracture properties of quasibrittle materials. If the size of the localized damage zone is smaller than the element, the overall tensile strength of the finite element would be governed by the minimum tensile strength of all potential damage zones within the element, which cannot be adequately described by either direct local projection or local averaging methods. For quasibrittle materials, the mapping method of random fields of material properties and the resulting probability distributions of constitutive properties of the finite element are strongly influenced by the damage pattern.

It has been well known that quasibrittle materials exhibit a strain-localization behavior, which has profound implications for finite element simulations. Over the years, various regularization methods have been developed to prevent spurious mesh dependence in deterministic FE analysis [3, 7, 8]. Recent studies have found that, for SFEM, energy regularization of the constitutive relationship alone is insufficient to mitigate the spurious mesh dependence in the predicted statistics of structural response [9,10]. Although these studies highlight the critical importance of relating the cumulative distribution functions (cdfs) of constitutive properties to the damage pattern, they neglect the spatial correlation of random material properties by imposing restrictions on the FE mesh size relative to the correlation length and fracture process zone (FPZ) width. These restrictions may not be applicable in all scenarios. Based on these findings, it has become clear that the mapping algorithm of random fields of material properties needs to be devised according to the damage pattern of the finite element. This study focuses on developing such a mechanism-based mapping method and examining its performance in

stochastic FE simulations of quasibrittle fracture.

2 CONSTITUTIVE MODEL

This study adopts a recently developed isotropic damage model with a general energy regularization scheme for tension-dominant failure [8, 10]. The stress-strain relationship is written as $\boldsymbol{\sigma} = f(\omega)\boldsymbol{C} : \boldsymbol{\epsilon}$, where $\boldsymbol{C}$ is the elastic stiffness tensor, ω is a scalar damage variable increasing from 0 (virgin state) to 1 (fully damaged state), $\boldsymbol{\epsilon}$ is the infinitesimal strain tensor, and $f(\omega)$ is a damage function which decreases monotonically from 1 to 0 as ω increases. We postulate a free energy function $Y(\omega, \boldsymbol{\epsilon})$, where the energy release (per unit thickness) of the finite element due to an increment amount of damage $\delta\omega$ is equal to $A_e \delta Y$, A_e = area of finite element. Consider a quadrilateral element, let h_1 be the width passing through the centroid in the direction of a principal vector $\vec{n}_e$, defined as the maximum principal strain direction at damage onset (Fig. 1a). We define element size h_2 in the orthogonal direction such that $A_e = h_1 h_2$. The balance between the energy released by damage and the energy expended for crack propagation can be written as

$$\frac{\partial Y}{\partial \omega} + \frac{n_b \widetilde{G}_f}{h_1} = 0 \qquad (1)$$

where $Y = \frac{1}{2}f(\omega)\widetilde{E}\bar{\epsilon}^2$, $\widetilde{G}_f$ = average value of fracture energies of n_b FPZs, $\widetilde{E}$ is the average Young modulus of the element, and $\bar{\epsilon} = \sqrt{\sum_{i=1}^{3}\langle\epsilon_i\rangle^2}$ (ϵ_i = principal strains, $\langle\cdot\rangle$ = Macaulay bracket) [11]. It has been suggested that the localization level of each finite element can be quantified based on the local damage patterns of the two adjacent elements aligned most closely with principal vector $\vec{n}_e$ [9]. For element i, the following localization parameter was recently proposed [10]:

$$\chi_1 = \left\langle 1 - \frac{\hat{\omega}_m + \hat{\omega}_n}{2\hat{\omega}_i} \right\rangle^{1/2} \qquad (2)$$

where $\hat{\omega}_k$ ($k = i, m, n$) denotes the representative damage level of element k. The representative damage level of element k is determined

as a weighted average of the damage values of the element itself and the two adjacent elements that are aligned closest to the direction of the principal vector of the element. For each finite element, the number of active FPZs is related to its localization parameter by

$$n_b = 1 + \left(\frac{h_1}{h_0} - 1\right) \left\{ 1 - \left[\frac{\langle \chi_1 - \chi_{t1} \rangle}{\chi_m - \chi_{t1}}\right]^\kappa \right\} \tag{3}$$

where h_0 is the FPZ width (a material characteristic length), and κ and χ_{t1} are constants. χ_{t1} determines the threshold value of χ_1 below which the element is deemed to experience a fully diffused damage pattern. κ describes the transitional behavior between the fully diffused damage case and the fully localized damage case in terms of χ_1. The constitutive model is completed by prescribing the form of damage function $f(\omega)$. In this study we use an $f(\omega)$ function which yields an exponential softening behavior under uniaxial tension [12]. The damage function is characterized by the tensile strength $\widetilde{f}_t$ and Young modulus $\widetilde{E}$ of the finite element.
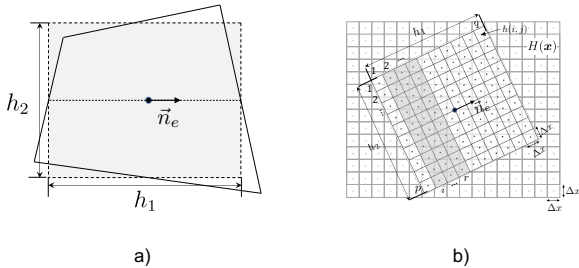

Figure 1: a) Definition of mesh size of a quadrilateral finite element, and b) a finite element laying over a random field of material property.

3 MODELING OF RANDOM CONSTITUTIVE PROPERTIES

Due to the heterogenous nature of quasibrittle materials, the material-point properties are expected to exhibit a considerable degree of spatial variability, which can mathematically be described by random fields. Here we consider these random fields to be homogenous and statistically independent. For material property H,

the corresponding random field $H(\boldsymbol{x})$ can be generated by using the power spectral density method [13, 14] if it is Gaussian. If $H(\boldsymbol{x})$ is non-Gaussian, we first generate a Gaussian random field and then transform it to the target non-Gaussian field [15].

Consider a finite element of size $h_1 \times h_2$ that lays over a random field $H(\boldsymbol{x})$, which is generated using a grid of size Δx aligned with the specimen's global coordinate system (Fig. 1b). The random values of H of all grids covered by the finite element are stored in a matrix $\boldsymbol{h}$ of size $p \times q$ using bilinear interpolation of the underlying random field, where $p,\ q =$ numbers of grids along h_2 and h_1 directions, respectively. The Young modulus of the finite element is taken as the average of the Young moduli of all the grids inside the finite element. By contrast, the mappings of tensile strength $\widetilde{f}_t$ and fracture energy $\widetilde{G}_f$ need to be tied to the damage pattern. Here we distinguish two scenarios of localized damage: Case 1) a localized damage band initiates inside the element, and Case 2) the localized damage forms inside the element due to the propagation of localized damage from an adjacent element. To differentiate these two cases, for finite element i, we propose the following parameter

$$\chi_2 = \max_j \left[\chi_{1j} \left(1 - |\vec{n}_e \cdot \vec{v}_{ij}| \right) \right] \tag{4}$$

where $\vec{v}_{ij}$ is a unit vector in the direction from the centroid of element i to that of its adjacent element j, and χ_{1j} is the value of χ_1 of element j.

For case I ($\chi_2 \leq \chi_{t2}$), the apparent tensile strength is equal to the minimum average tensile strength of all the potential damage bands in the element. The average tensile strength of a potential damage band is calculated by averaging the random tensile strengths of the grids that are covered by the damage band. Once the damage band with the minimum average tensile strength is identified, the apparent fracture energy of the finite element is thus the average fracture energy of that particular damage band.

For case II ($\chi_2 > \chi_{t2}$), the damage band in the current element is formed as a result of the

3

propagation of the localized damage band from the adjacent element. Consider the adjacent element j has a localized damage, where the centroid of this damage band is denoted by $\vec{x}_{b_j}$. The centroid of the damage band in the current element i is located at the intersection between the line emanating from the centroid $\vec{x}_{b_j}$ in the direction of the principal vector $\vec{n}_e^j$ of element j and the centerline of the current element in the direction of its principal vector (Fig. 2). Once the location of the damage band is determined, the apparent tensile strength and fracture energy of the current element are computed as an average over this particular damage band.
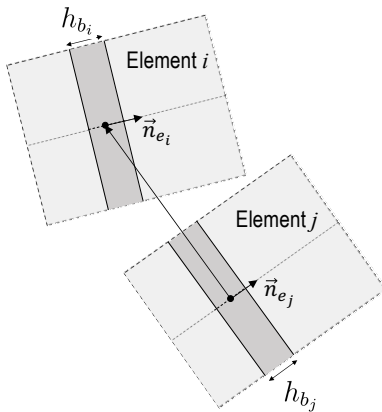

Figure 2: Identification of the location of a propagating localized damage band.

4 NUMERICAL STUDIES

The present model is applied to simulate the failure behavior of three-point and four-point bend specimens made of dense alumina ceramic. The specimens are loaded in a displacement-controlled mode, and a sufficiently large number of realizations (approximately 400) are used to ensure convergence of the second order statistics of peak load. In this study, we consider that E and G_f follow a Gaussian distribution, and f_t follows the Gauss-Weibull distribution. The spatial variations of E, G_f, and f_t are characterized by squared exponential covariance functions [16]. In the analysis, we consider three different correlation lengths: $l_a = h_0/4, h_0/2$, and h_0.

The stochastic simulations are conducted in the open-source FEM software OOFEM with a Matlab interface for performing the mapping algorithm. To investigate the mesh insensitivity, three different element widths ($h_0, 2h_0$, and $4h_0$) are used in the simulation. As a comparative study on mesh sensitivity, we consider three mapping methods: 1) the present method, 2) local mapping method, and 3) local averaging method. When comparing the proposed mapping method to the local mapping and local averaging methods, the same mechanism-based energy regularization described by Sec. 2 is used for all simulation cases.

5 RESULTS AND DISCUSSION

For all tested CLs, the mean peak loads $\bar{P}_m$ of the four-point bend beams predicted with the three mapping methods are nearly insensitive to the mesh size (Fig. 3). This is due to the present energy regularization scheme, which is applied to all three mapping methods. In Fig. 4a, it is seen that the standard deviation of peak load δ_P predicted by the local mapping method increases with the mesh size. This result can be explained from the damage pattern. Upon loading, a damage zone of a considerable size is first formed. At the peak load, a localized damage band (i.e. macrocrack) forms and initiates from a random location inside this damage zone. As the mesh size increases, there are a fewer number of elements in the damage zone. Since the local mapping method uses the fixed cdfs of apparent tensile strength and fracture energy, a decrease in the number of elements in the damage zone leads to an increasing variability in energy dissipation.

Fig. 4a also shows that, as the CL increases, the mesh dependence gets less pronounced. For a larger CL value, each finite element exhibits less spatial randomness of material property. Thus, the statistics of constitutive properties become less dependent on the element size. Such a behavior is a general trend, which is also seen in the simulations of beams of other geometries for all three mapping methods. In Fig. 4b, it is seen that the local average method yields a less mesh-dependent δ_P. This is because, the

local average method gives the correct mapping during the early loading stage since the beam experiences a diffused damage pattern. Nevertheless, even though the result of local average method does not exhibit strong mesh dependence, the method does not correspond to the correct damage pattern. Fig. 4c presents the results of the present method. It is seen that the method yields a relatively mesh-insensitive standard deviation of peak load across all tested CL values.
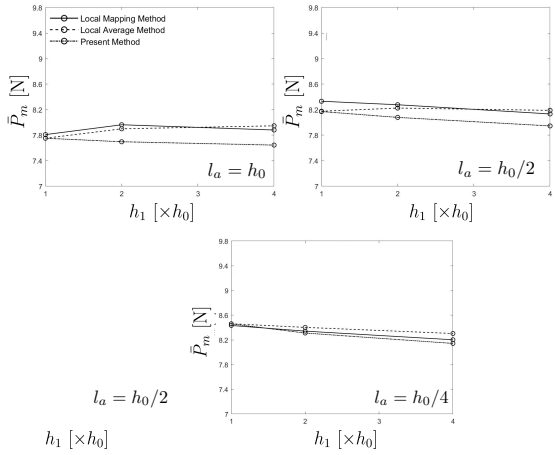

Figure 3: Mean peak loads of unnotched four-point bend beam simulated using different mesh sizes and different CLs.

For all three mapping methods, the simulated mean peak loads of the notched three-point bend beams are mesh insensitive (Fig. 5). In contrast to the case of unnotched three-point bend beams, Fig. 6a shows that the simulated δ_P of notched beam using the local mapping method does not exhibit strong mesh dependence. As loading proceeds, fully localized damage propagates upwards from the notch tip. At peak load, several elements along the ligament are damaged. Due to damage propagation, the locations of the damage bands inside these elements are deterministic. The apparent tensile strength $\widetilde{f}_t$ and fracture energy $\widetilde{G}_f$ are equal to the average tensile strength and fracture energy of one damage band. Consequently, the statistics of $\widetilde{f}_t$ and $\widetilde{G}_f$ are independent of the element
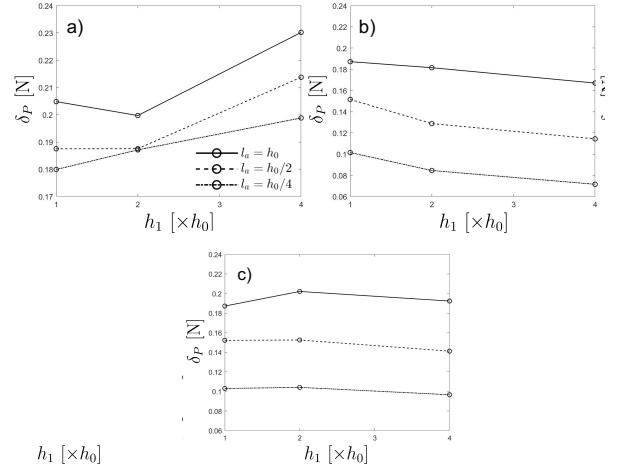
size.

Figure 4: Standard deviations of the peak load of unnotched four-point bend beam simulated using (a) local mapping method, (b) local averaging method, and (c) present method.
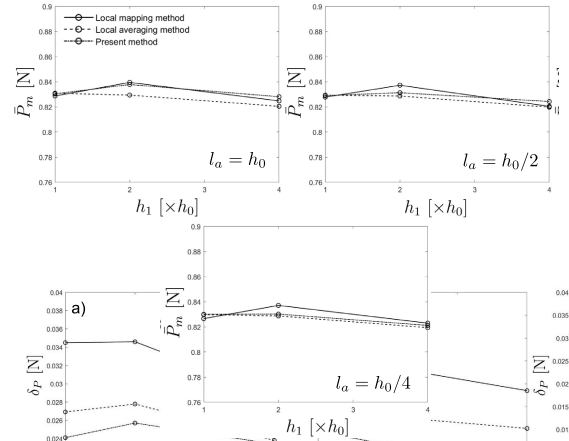

Figure 5: Mean peak loads of notched three-point bend beam simulated using different mesh sizes and different CLs.

By contrast, the standard deviation δ_P calculated by the local average method exhibits a strong mesh dependence (Fig. 6b). As mentioned earlier, the local average method predicts that the statistical variation of $\widetilde{f}_t$ and $\widetilde{G}_f$ decreases as the mesh size increases. However,

the localized damage pattern of the notched beam dictates that the statistics of $\widetilde{f}_t$ and $\widetilde{G}_f$ should not be mesh dependent. As shown in Fig. 6c, the present method yields a nearly mesh-insensitive result for δ_P. In the simulation, parameter χ_2 of the elements along the ligament takes its maximum value as soon as damage occurs in the first element above the notch tip.
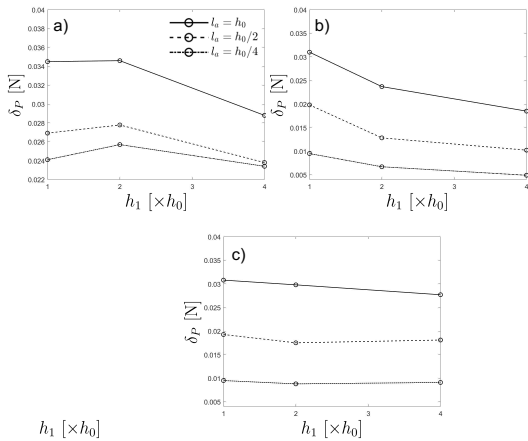

Figure 6: Standard deviations of the peak load of notched three-point bend beam simulated using (a) local mapping method, (b) local averaging method, and (c) present method.

6 CONCLUSIONS

Quasibrittle structures typically display complex damage patterns and failure behaviors, leading to intricate mesh dependence in stochastic FE simulations. It has been shown that the energy regularization scheme is inadequate for addressing the mesh dependence of second-order failure statistics. Mesh sensitivity diminishes when the correlation length of the random fields of material properties is large compared to the FE mesh size.

The core issue is how to project the continuous random fields of material properties onto the FE mesh. This study develops a mechanism-based mapping method that updates the mapping algorithm according to the evolving damage pattern during the loading process. A key implication is that the resulting

statistics of the constitutive properties of the finite element can vary with mesh size, governed by the damage pattern.

Numerical studies indicate that local mapping and local average methods are insufficient for reducing mesh dependence of the failure load statistics. In contrast, the present model offers a robust solution for mitigating mesh dependence across various structural geometries with different failure mechanisms. The effectiveness of this model relies on the connection between the damage pattern and the mapping of the random fields of material properties.

REFERENCES

[1] Z. P. Bazant and S. D. Pang, "Mechanics based statistics of failure risk of quasibrittle structures and size effect on safety factors," *Proc. Nat'l. Acad. Sci., USA*, vol. 103, pp. 9434–9439, 2006.

[2] J.-L. Le, Z. P. Bažant, and M. Z. Bazant, "Unified nano-mechanics based probabilistic theory of quasibrittle and brittle structures: I. strength, crack growth, lifetime and scaling," *J. Mech. Phys. Solids*, vol. 59, pp. 1291–1321, 2011.

[3] Z. P. Bažant and J.-L. Le, *Probabilistic Mechanics of Quasibrittle Structures: Strength, Lifetime, and Size Effect*. Cambridge, U.K.: Cambridge University Press, 2017.

[4] E. Vanmarcke, *Random Fields Analysis and Synthesis*. Singapore: World Scientific Publishers, 2010.

[5] E. Vanmarcke and M. Grigoriu, "Stochastic finite element analysis of simple beams," *J. Engrg. Mech. ASCE*, vol. 109, pp. 1203–1214, 1983.

[6] A. der Kiureghian and J. B. Ke, "The stochastic finite element method in structural reliability," *Prob. Engrg. Mech.*, vol. 3, pp. 83–91, 1988.

[7] Z. P. Bažant and M. Jirásek, "Nonlocal integral formulations of plasticity and damage: Survey of progress," vol. 128, no. 11, pp. 1119–1149, 2002.

[8] A. Gorgogianni, J. Eliáš, and J.-L. Le, "Mechanism-Based Energy Regularization in Computational Modeling of Quasibrittle Fracture," *J. Appl. Mech.*, vol. 87, no. 9, 2020.

[9] J.-L. Le and J. Eliáš, "A probabilistic crack band model for quasibrittle fracture," *J. Appl. Mech., ASME*, vol. 83, no. 5, p. 051005, 2016.

[10] A. Gorgogianni, J. Elias, and J.-L. Le, "Mesh objective stochastic simulations of quasibrittle fracture," *J. Mech. Phys. Solids*, vol. 159, p. 104745, 2022.

[11] J. Mazars, *Application de la mécanique de l'endommagement au comportement non linéaire et à la rupture du béton de structure*. PhD thesis, University of Paris VI, Paris, France, 1984.

[12] J.-Y. Wu and V. P. Nguyen, "A length scale insensitive phase-field damage model for brittle fracture," *J. Mech. Phys. Solids*, vol. 119, pp. 20–42, 2018.

[13] M. Shinozuka and G. Deodatis, "Simulation of stochastic processes by spectral representation," *Appl. Mech. Rev.*, vol. 44, no. 4, pp. 191–204, 1991.

[14] M. Shinozuka and G. Deodatis, "Simulation of multi-dimensional gaussian stochastic fields by spectral representation," *Appl. Mech. Rev.*, vol. 49(1), pp. 29–53, 1996.

[15] F. Yamazaki and M. Shinozuka, "Digital generation of non-gaussian stochastic fields," *J. Eng. Mech.*, vol. 114(7), pp. 1183–1197, 1988.

[16] P. Grassl and Z. P. Bažant, "Random lattice-particle simulation of statistical size effect in quasi-brittle structures failing at crack initiation," *J. Engrg. Mech., ASCE*, vol. 135, no. 2, pp. 85–92, 2009.